Chapter 3

Seismic Engineering: The Structural Model

3.1 Introduction

In the following chapters we show different techniques to reduce building response when excited by earthquakes. To this end first a two-dimensional linear model of a multistory building was developed. Then hysteretic characteristics were added to the model. To control the response of the structure we modeled a tuned mass damper (TMD) located on the roof of the building. Such devices provide a good passive reduction. Once the mass damper is properly tuned, active control is added to improve the already efficient passive controller. This is achieved by means of a neural network.

3.2 The Structural Model

We model the building with a classic shear-beam representation. The coupled equations of motion of the system with N_f stories and an active tuned mass damper can be written in the following general form:

$$\mathbf{M}\,\ddot{\mathbf{z}}(t) + \mathbf{C}\,\dot{\mathbf{z}}(t) + \mathbf{K}\,\mathbf{z}(t) = \mathbf{M}\,\mathbf{r}\,\ddot{x}_g(t) + \mathbf{h}\,u_c(t) \tag{3.1}$$

where **z** is the $N_d \times 1$ vector of relative displacements of each degree of freedom with respect to the base, and N_d represents the number of degrees of freedom of the building-TMD system ($N_d = N_f + 1$). The acceleration $\ddot{x}_g$ is the seismic excitation. The $N_d \times N_d$ matrices **M**, **C** and **K**, are the mass, damping and stiffness matrices of the system, respectively. The $N_d \times 1$ vector **r** denotes the influence vector of the ground motion. The second term on the right-hand side incorporates the effect of the control force *u* in the equations of motion by using the $N_d \times 1$ location vector **h** to specify the position of the actuation device.

The mass, stiffness, and viscous damping coefficients of the TMD are denoted by m_a, k_a and c_a, respectively. The characteristics of the tuned mass damper are defined by the tuning, mass, and damping ratios as follows:

$$f_r = \frac{\omega_a}{\omega_1}; \quad m_r = \frac{m_a}{m_t}; \quad \xi_a = \frac{c_a}{2\, m_a\, \omega_a} \tag{3.2}$$

where ω_a and ω_1 indicate the fundamental frequencies of the TMD and the structure, respectively, and m_t denotes the total mass of the building.

In Figure 3-1 a ten-story building with a TMD over the tenth floor is represented schematically, where $z_i(t)$ is the displacement (in the time domain) of each floor *i*, and *h* is the coordinate perpendicular to the ground.

We have also added hysteretic characteristics based on the Bouc-Wen model [6**,** 62**,** 64**,** 97]. For this case the stiffness force given by the hysteretic structure can be computed as

$$\mathbf{f}(\mathbf{d}, \boldsymbol{\zeta}) = \boldsymbol{\alpha}\, \mathbf{K}_h\, \mathbf{d} + (\mathbf{I} - \boldsymbol{\alpha})\, \mathbf{K}_h\, \boldsymbol{\zeta} \tag{3.3}$$

where **f** and **d** are the restoring force and corresponding inter-story deformation vector; $\boldsymbol{\zeta}$ is the hysteretic auxiliary variable of the force, $\mathbf{K}_h$ is a modified stiffness matrix (which we describe below), and $\boldsymbol{\alpha}$ is a vector with positive elements. Vectors **f**, **d,** $\boldsymbol{\zeta}$ and $\boldsymbol{\alpha}$ are N_d dimensional vectors. The hysteretic variable is defined by the following first-order, nonlinear differential equation $\dot{\boldsymbol{\zeta}} = \mathbf{g}(\dot{\mathbf{d}}, \boldsymbol{\zeta})$, which can be expressed as:

$$\dot{\zeta}_i = \dot{d}_i - \frac{1}{2}\frac{|\zeta_i|^{n-1}}{|\zeta_i^u|^n}\left(|\dot{d}_i|\,\zeta_i + \dot{d}_i\,|\zeta_i|\right) \qquad \text{for} \quad i = 1 \ldots N_d \tag{3.4}$$

where the exponent n controls the shape of the hysteresis curve, and ζ_i^u denotes the ultimate value of the hysteretic variable.

To complete the hysteretic model we need to replace the linear stiffness term given by $\mathbf{K}\,\mathbf{z}(t)$ in equation (3.1), by the hysteretic restoring force given by equation (3.3). Prior to this step, we make a linear transformation of equation (3.1) such that we obtain a new stiffness matrix $\mathbf{K}_h$ which has different-from-zero elements only in the main diagonal. To this end we express $\mathbf{z}$ in terms of the corresponding interstory drifts, $\mathbf{d}$, according to:

$$\mathbf{z} = \mathbf{T}\,\mathbf{d} \tag{3.5}$$

where **T** is a $N_d \times N_d$ matrix of the form

$$\mathbf{T} = \begin{bmatrix} 1 & 1 & \cdots & 1 \\ 0 & 1 & \cdots & 1 \\ \vdots & \vdots & \ddots & \vdots \\ 0 & 0 & \cdots & 1 \end{bmatrix} \tag{3.6}$$

Substituting equation (3.5) into equation (3.1) we get,

$$\mathbf{M}\left(\mathbf{T}\,\ddot{\mathbf{d}}\right)+\mathbf{C}\left(\mathbf{T}\,\dot{\mathbf{d}}\right)+\mathbf{K}\left(\mathbf{T}\,\mathbf{d}\right)=-\mathbf{r}\,\ddot{x}_g+\mathbf{h}\,u_c(\mathbf{y}) \tag{3.7}$$

Premultiplying both sides of equation (3.7) by $\mathbf{T}^T$ we get,

$$\mathbf{M}_h\,\ddot{\mathbf{d}}+\mathbf{C}_h\,\dot{\mathbf{d}}+\mathbf{K}_h\,\mathbf{d}=-\mathbf{r}_h\,\ddot{x}_g+\mathbf{h}_h\,u_c(\mathbf{y}) \tag{3.8}$$

where

$$\mathbf{M}_h=\mathbf{T}^T\mathbf{M}\,\mathbf{T} \tag{3.9}$$

$$\mathbf{C}_h=\mathbf{T}^T\mathbf{C}\,\mathbf{T} \tag{3.10}$$

$$\mathbf{K}_h=\mathbf{T}^T\mathbf{K}\,\mathbf{T} \tag{3.11}$$

$$\mathbf{r}_h=\mathbf{T}^T\mathbf{r} \tag{3.12}$$

$$\mathbf{h}_h=\mathbf{T}^T\mathbf{h} \tag{3.13}$$

The new stiffens matrix $\mathbf{K}_h$ has non-zero elements only in the diagonal, and matrices $\mathbf{M}_h$ and $\mathbf{C}_h$ are in general fully populated matrices. We are finally ready to replace the linear stiffness term $\mathbf{K}\,\mathbf{z}(t)$ by the hysteretic restoring term $\mathbf{f}(\mathbf{d},\boldsymbol{\zeta})$ given by equation (3.3). The resulting equations of motion can then be written as:

$$\mathbf{M}_h\,\ddot{\mathbf{d}} + \mathbf{C}_h\,\dot{\mathbf{d}} + \mathbf{f}(\mathbf{d},\boldsymbol{\zeta}) = -\,\mathbf{r}_h\,\ddot{x}_g + \mathbf{h}_h\,u_c(\mathbf{y}) \tag{3.14}$$

$$\dot{\boldsymbol{\zeta}} = \mathbf{g}(\dot{\mathbf{d}},\boldsymbol{\zeta}) \tag{3.15}$$

3.3 Input Data and Numerical Examples

In Chapters 6 and 7, we discuss how to reduce the vibrations of different buildings when they are subjected to seismic excitations. We use three ground accelerations records as the testing and validating inputs: the El Centro (1941), San Fernando (1971) and Loma Prieta (1989) earthquakes. They are shown in figures 3-2, 3-3 and 3-4. There each earthquake is normalized with a maximum peak acceleration of 0.3*g*.

As we discuss in chapters 6 and 7, we apply artificially generated earthquakes to train the controller. In all we use ten training-datum ground motions in this dissertation. They are plotted in Figure 3-5, parts *a* to *j*.

The spectrum distribution of El Centro, San Fernando and Loma Prieta earthquakes are shown in Figures 3-6, 3-7, and 3-8, respectively. In each of these pictures, the average of the synthesized response spectrum is also displayed. The spectrum distribution of the synthesized earthquakes is shown in Figure 3-9.

To show the hysteretic characteristics of the model we use a six-story shear-building model with uniform mass, stiffness and strength properties. The first natural period is about 0.61*sec*. A modal damping ratio of 3% is assumed for all modes to define the damping matrix. In Figure 3-10 we show the hysteretic cycle of the base shear, normalized with the total weight of the building, versus base drift for the example building when excited for the El Centro ground motion. In parts *a* and *b* we show the uncontrolled and controlled cases, respectively. We see that, for the controlled case, the hysteretic cycle is smaller, in proportion to the reduction of the base shear. In Figure 3-11 we show the corresponding results when the building is excited with the San Fernando ground motion. Analogous results as for El Centro earthquake were obtained.

In Figure 3-12 we show the elastic and hysteretic peak relative displacements of each floor for El Centro ground motion. The displacements are normalized with the corresponding uncontrolled cases. We see that the elastic peaks are larger than the corresponding hysteretic peaks for all floors. This evidences hysteretic dissipation. In Figure 3-13 we show the peak absolute accelerations of each floor. Hysteretic dissipation is also observed.

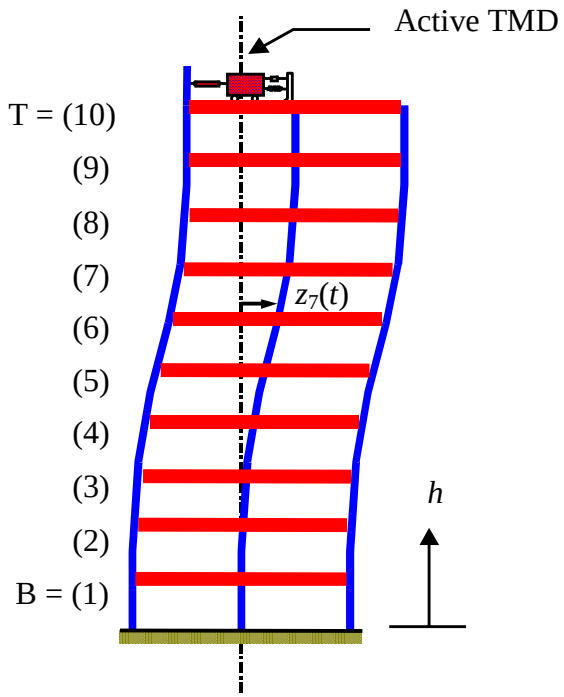

Figure 3-1: Schematic representation of a building equipped with an active TMD.

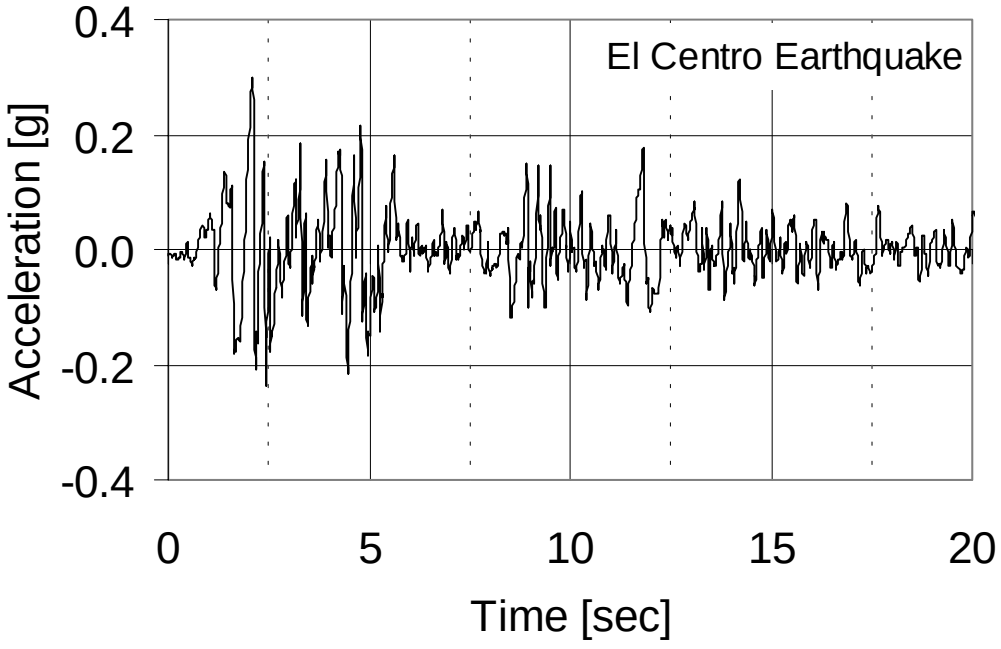

Figure 3-2: El Centro ground motion.

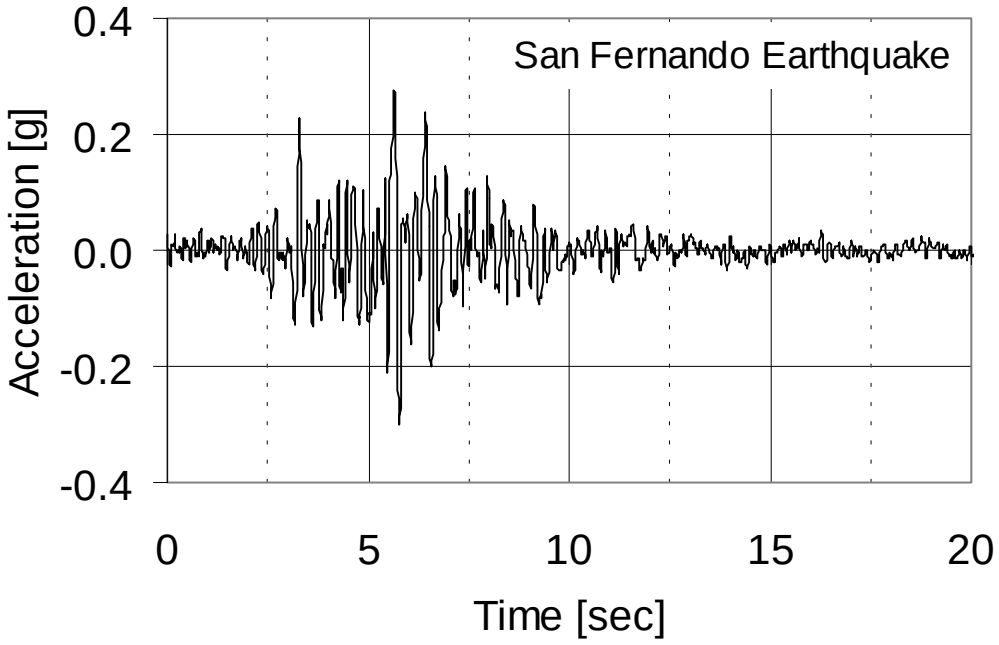

Figure 3-3: San Fernando ground motion.

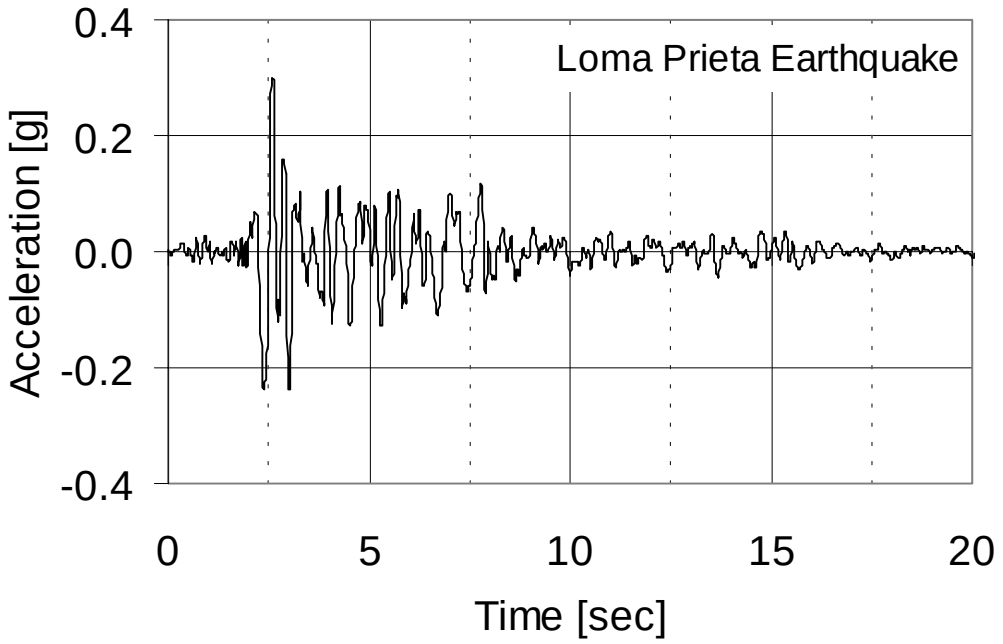

Figure 3-4: Loma Prieta ground motion.

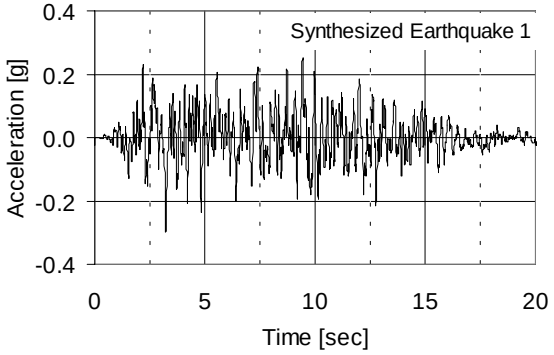
Synthesized Earthquake 1
Acceleration [g]
0.4
0.2
0.0
-0.2
-0.4
0
5
10
15
20
Time [sec]

(a)

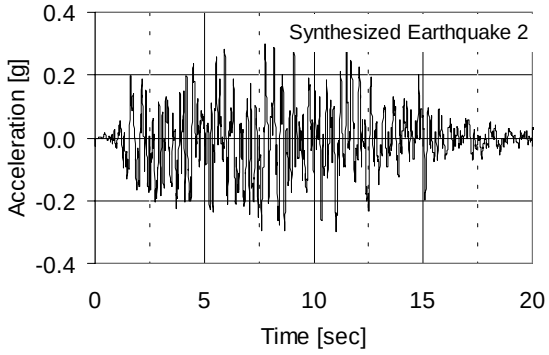
Synthesized Earthquake 2
Acceleration [g]
0.4
0.2
0.0
-0.2
-0.4
0
5
10
15
20
Time [sec]

(b)

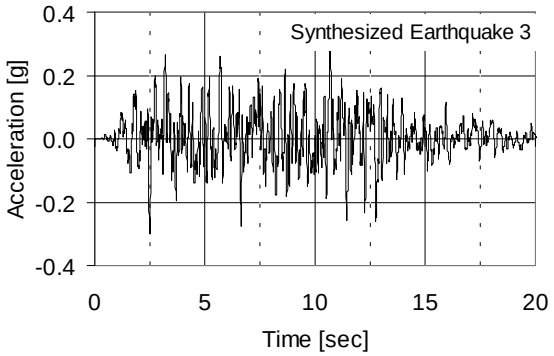
Synthesized Earthquake 3
Acceleration [g]
0.4
0.2
0.0
-0.2
-0.4
0
5
10
15
20
Time [sec]

(c)

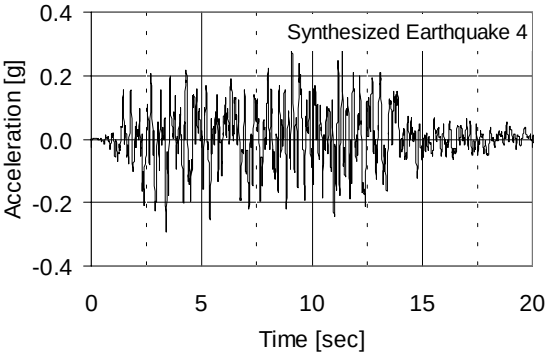
Synthesized Earthquake 4
Acceleration [g]
0.4
0.2
0.0
-0.2
-0.4
0
5
10
15
20
Time [sec]

(d)

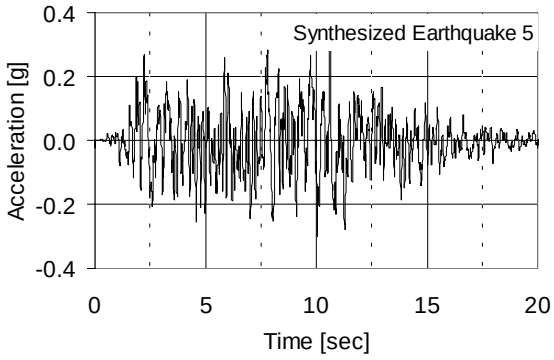
Synthesized Earthquake 5
Acceleration [g]
0.4
0.2
0.0
-0.2
-0.4
0
5
10
15
20
Time [sec]

(e)

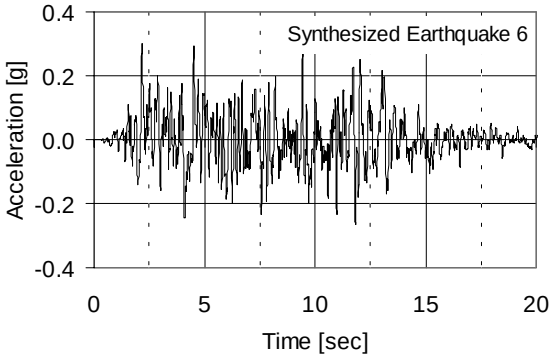

(f)

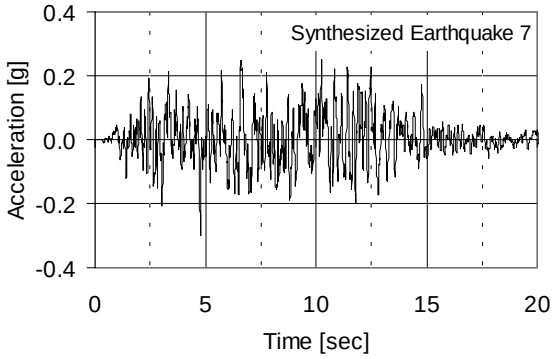

(g)

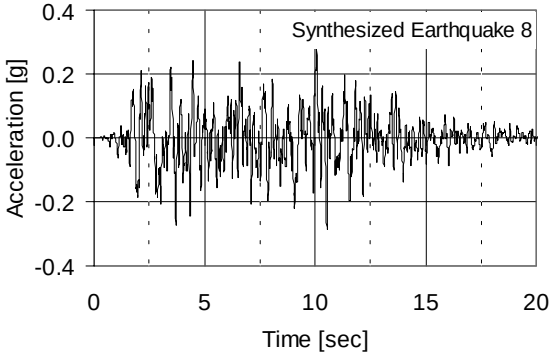

(h)

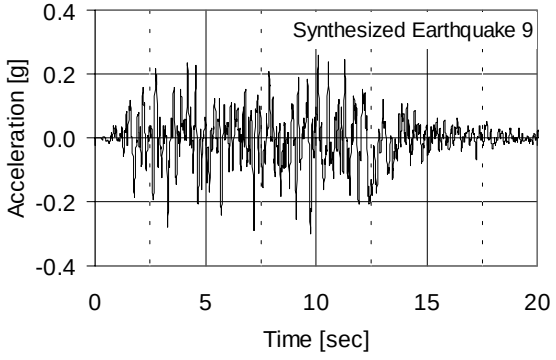

(i)

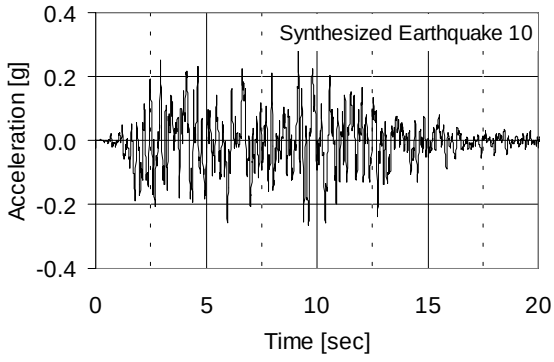

(j)

Figure 3-5: Ground motions for 10 artificially generated excitations.

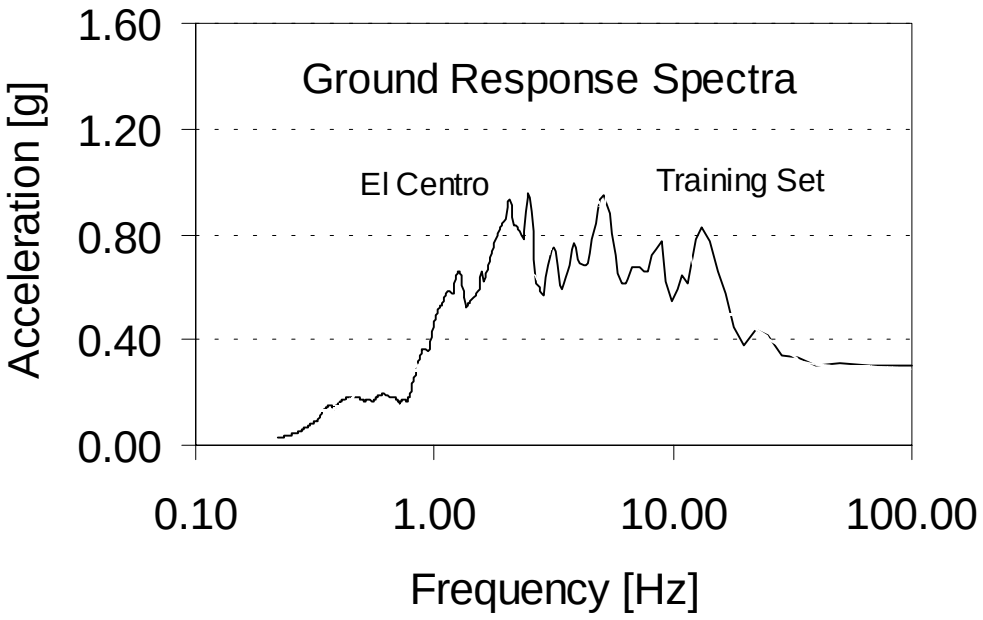

Figure 3-6: Ground response spectrum of the El Centro earthquake (strong line), and of the average spectrum of the 10 synthesized earthquakes (thin line).

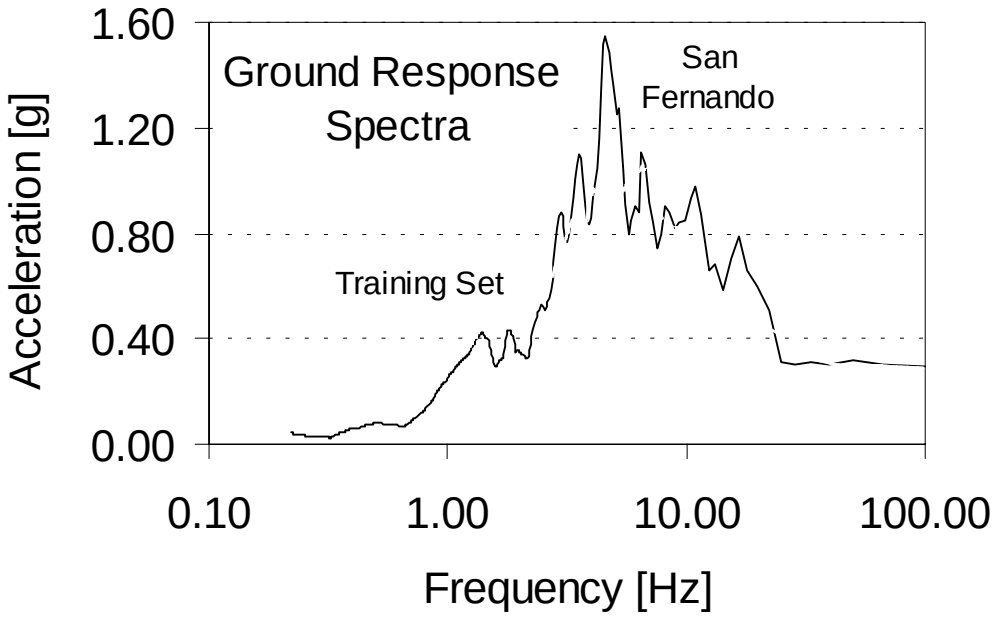

Figure 3-7: Ground response spectrum of the San Fernando earthquake (strong line), and of the average spectrum of the 10 synthesized earthquakes (thin line).

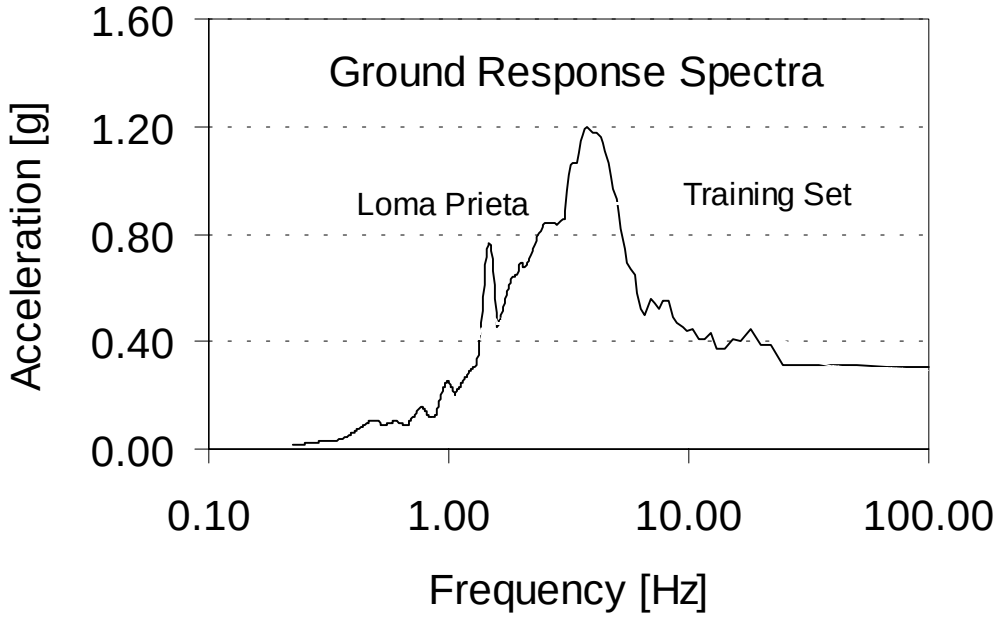

Figure 3-8: Ground response spectrum of the Loma Prieta earthquake (strong line), and of the average spectrum of the 10 synthesized earthquakes (thin line).

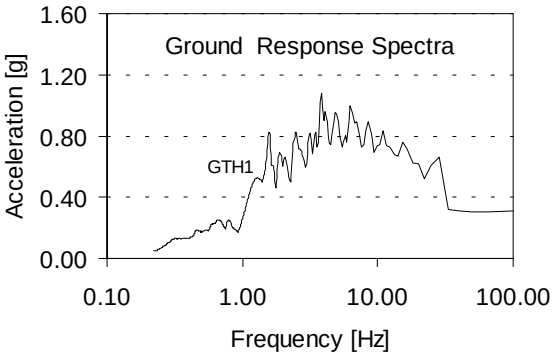
Ground Response Spectra
GTH1
Acceleration [g]
1.60
1.20
0.80
0.40
0.00
0.10
1.00
10.00
100.00
Frequency [Hz]

(a)

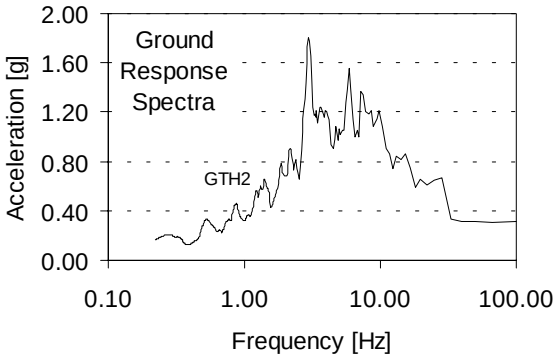
Ground
Response
Spectra
GTH2
Acceleration [g]
2.00
1.60
1.20
0.80
0.40
0.00
0.10
1.00
10.00
100.00
Frequency [Hz]

(b)

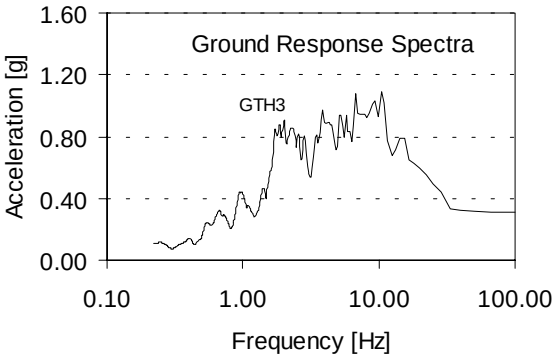
Ground Response Spectra
GTH3
Acceleration [g]
1.60
1.20
0.80
0.40
0.00
0.10
1.00
10.00
100.00
Frequency [Hz]

(c)

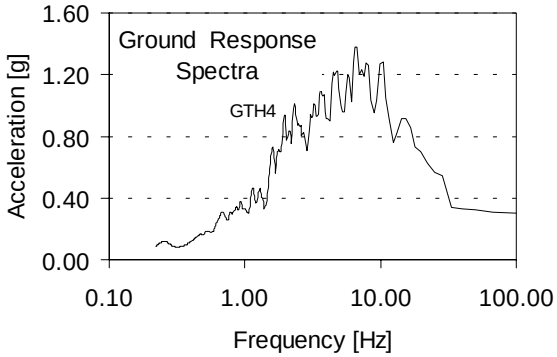
Ground Response
Spectra
GTH4
Acceleration [g]
1.60
1.20
0.80
0.40
0.00
0.10
1.00
10.00
100.00
Frequency [Hz]

(d)

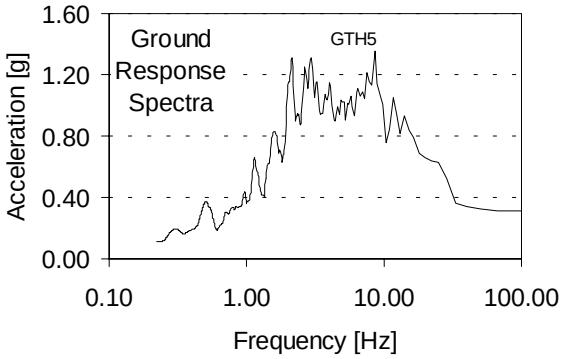
Ground
Response
Spectra
GTH5
Acceleration [g]
1.60
1.20
0.80
0.40
0.00
0.10
1.00
10.00
100.00
Frequency [Hz]

(e)

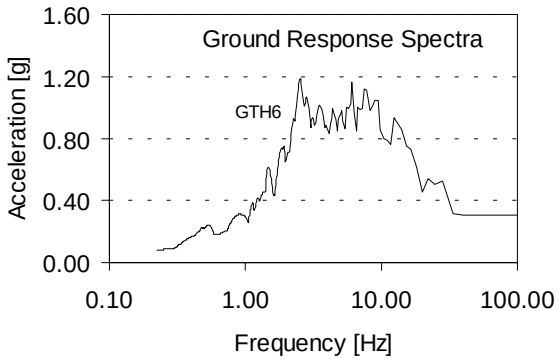

(f)

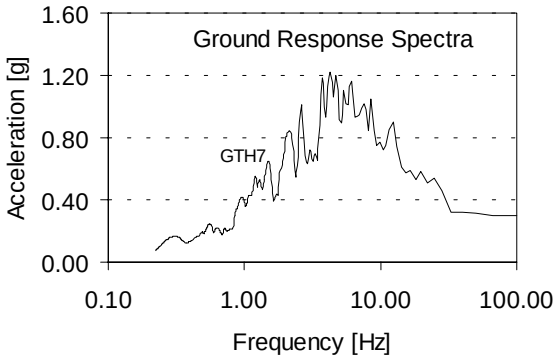

(g)

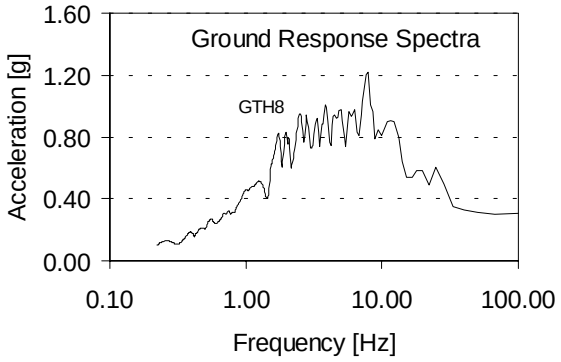

(h)

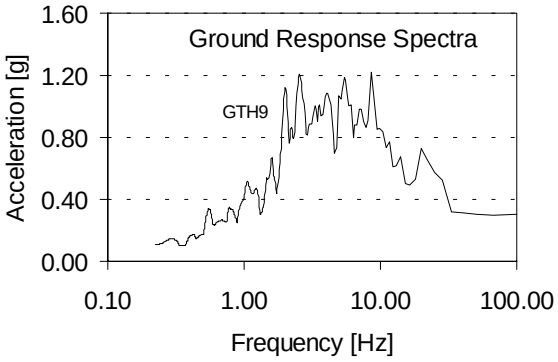

(i)

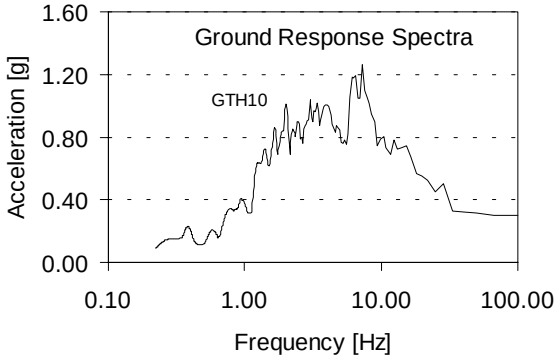

(j)

Figure 3-9: Ground response spectra for the 10 synthesized earthquakes (GTH= ground time histories).

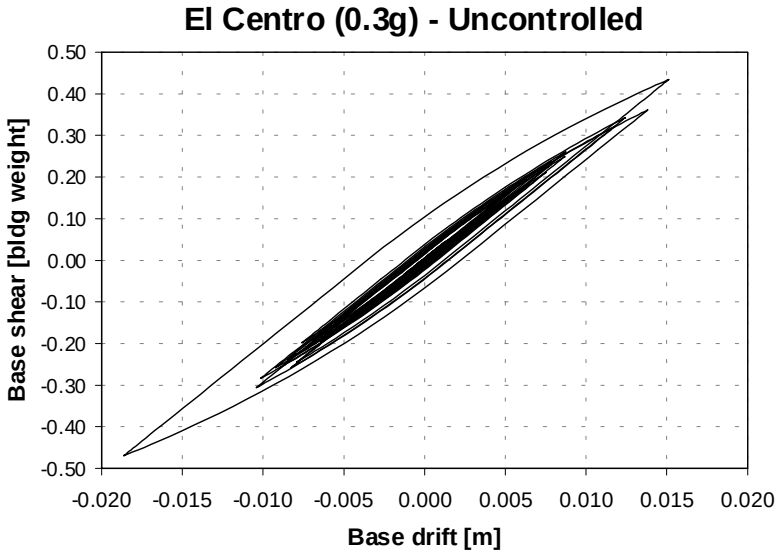

(a)

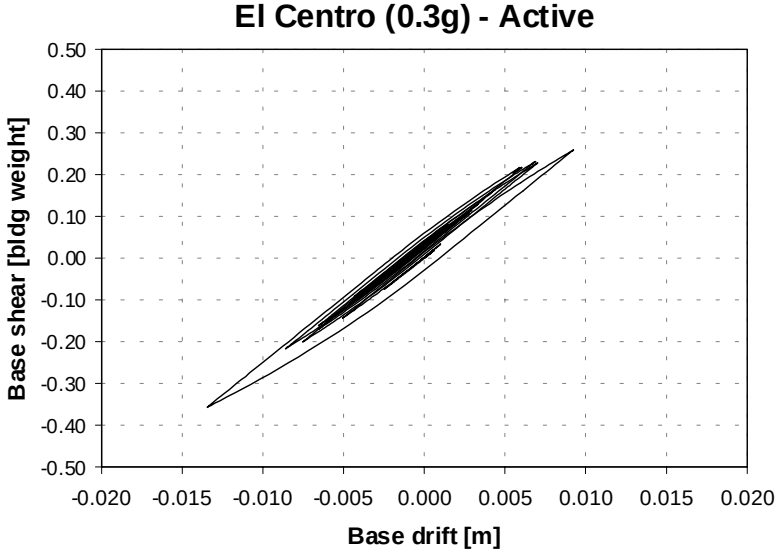

(b)

Figure 3-10: Hysteretic cycle of base shear versus base drift for a six-story building. Part *a*, no control; part *b*, active control. El Centro ground motion.

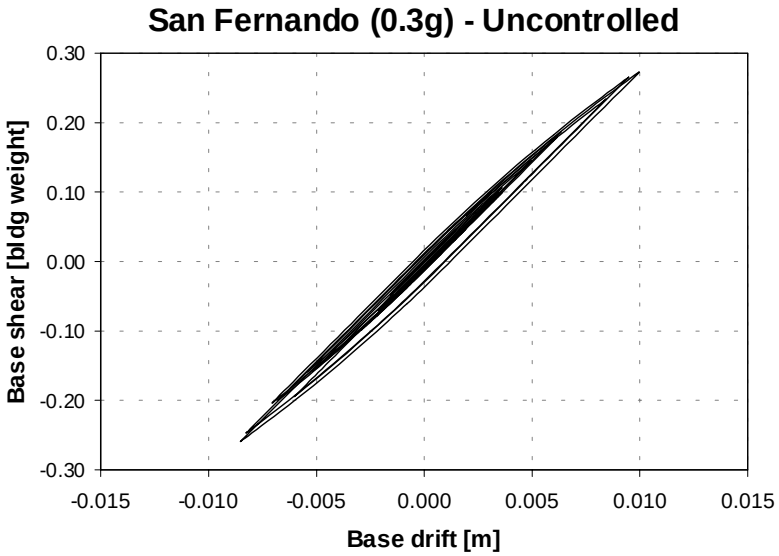

(a)

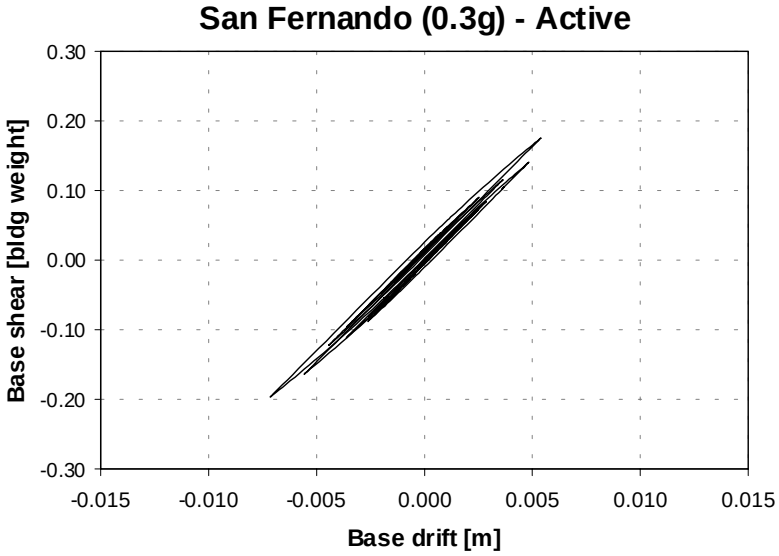

(b)

Figure 3-11: Hysteretic cycle of base shear versus base drift for a six-story building. Part *a*, no control; part *b*, active control. San Fernando ground motion.

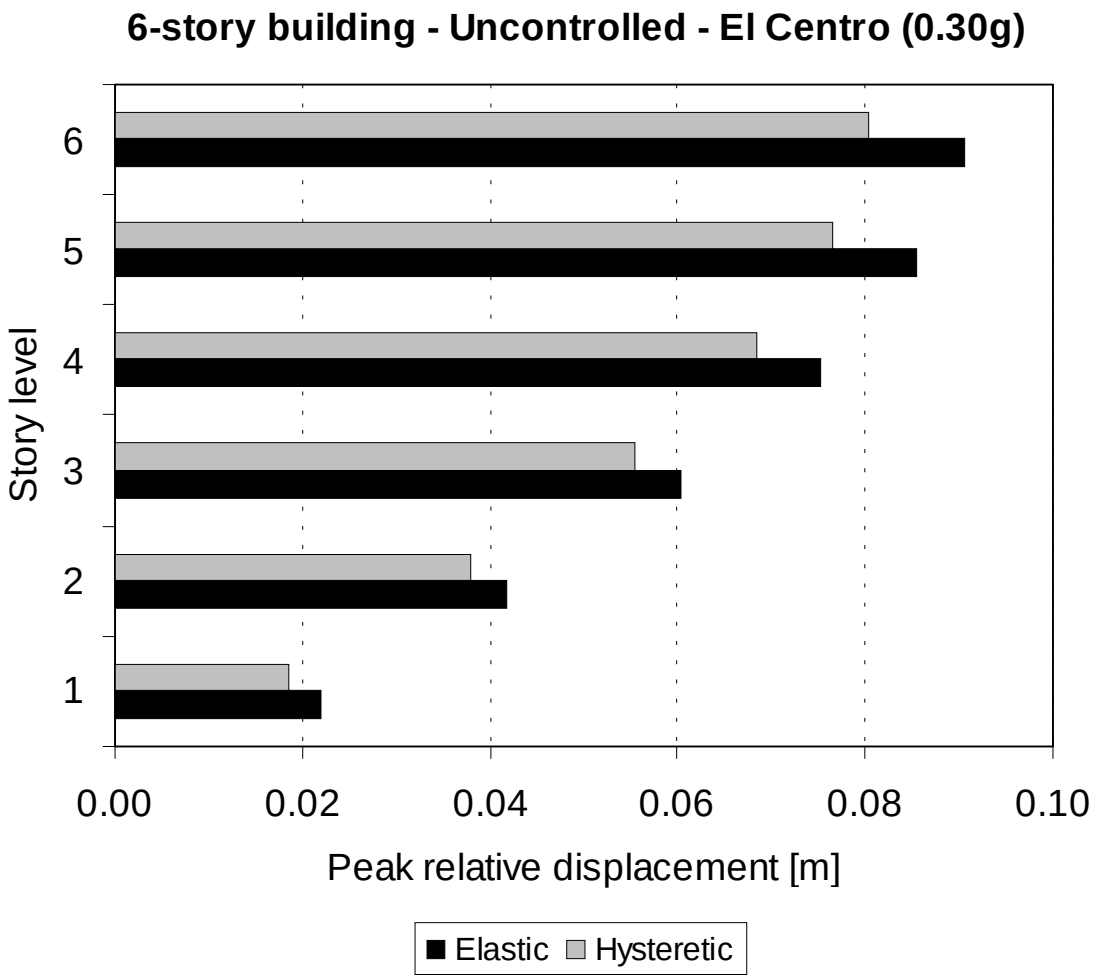

Figure 3-12: Elastic and hysteretic peak relative displacements for a six-story building. El Centro ground motion.

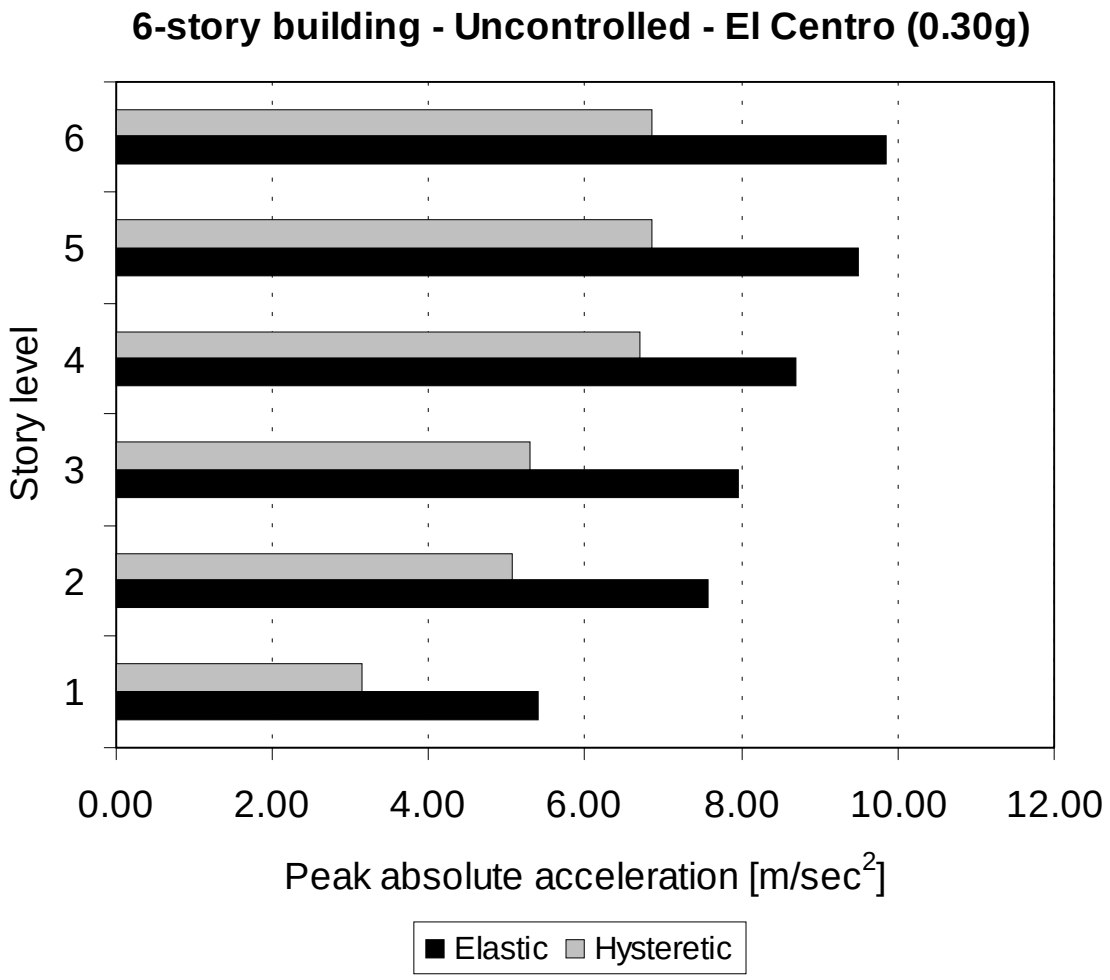

Figure 3-13: Elastic and hysteretic peak absolute accelerations for a six-story building. El Centro ground motion.